The Journal of Headache and Pain

RESEARCH

Open Access

Phasic perfusion dynamics among migraine subtypes: a multimodel arterial spin labeling investigation

Chia-Hung Wu[1,2], Pei-Lin Lee[3], Yen-Feng Wang[2,4,5], Jiing-Feng Lirng[1,2], Shu-Ting Chen[1,2], Chung-Jung Lin[1,2], Shuu-Jiun Wang[2,4,5*†], Kun-Hsien Chou[5,6*†] and Shih-Pin Chen[2,4,5,7,8*†]

Abstract

Background Migraine-related perfusion changes are documented but inconsistent across studies due to limited sample size and insufficient phenotyping. The phasic and spatial dynamics across migraine subtypes remains poorly characterized. This study aimed to determine spatiotemporal dynamics of gray matter (GM) perfusion in migraine.

Methods We prospectively recruited episodic (EM) and chronic migraine (CM) patients, diagnosed with the International Headache Society criteria and healthy controls (HCs) between 2021 and 2023 from the headache center in a tertiary medical center, and adjacent communities. Magnetic resonance (3-tesla) arterial spin labeling (ASL) was conducted for whole brain cerebral blood flow (CBF) in all participants. The voxel-wise and whole brain gray matter (GM) CBF were compared between subgroups. Spatial pattern analysis of CBF and its correlations with headache frequency were investigated regarding different migraine phases and subtypes. Sex- and age-adjusted voxel-wise and whole brain GM comparisons were performed between HCs and different EM and CM phases. Spatial pattern analysis was conducted by CBF clusters with phasic differences and spin permutation test. Correlations between headache frequency and CBF were investigated regarding different EM and CM phases.

Results Totally 344 subjects (172 EM, 120 CM, and 52 HCs) were enrolled. Higher CBF in different anatomical locations was identified in ictal EM and CM. The combined panels of the specific locations with altered CBF in ictal EM on receiver operating characteristic curve analysis demonstrated areas under curve of 0.780 (vs. HCs) and 0.811 (vs. preictal EM). The spatial distribution of ictal-interictal CBF alteration of EM and CM were not correlated with each other ($p = 0.665$; $r = -0.018$). Positive correlations between headache frequency and CBF were noted in ictal EM and CM regarding whole GM and specific anatomical locations.

†Shuu-Jiun Wang, Kun-Hsien Chou and Shih-Pin Chen contributed equally to this work.

*Correspondence:
Shuu-Jiun Wang
sjwang@vghtpe.gov.tw
Kun-Hsien Chou
dargonchow@gmail.com
Shih-Pin Chen
chensp1977@gmail.com

Full list of author information is available at the end of the article

Conclusions Patients with migraine exhibited unique spatiotemporal CBF dynamics across different phases and distinct between subtypes. The findings provide neurobiological insights into how selected anatomical structures engage in a migraine attack and adapt to plastic change of repeated attacks along with chronicity.

Keywords Migraine, Cerebral blood flow (CBF), Arterial spin labeling (ASL), Magnetic resonance imaging (MRI), Headache frequency, Ictal

Background

Migraine is a primary headache disease that affects approximately 14–15% of the population globally [1] and leads to substantial socioeconomic burdens [2]. According to the International Classification of Headache Disorders, 3rd edition (ICHD-3), migraines are classified into episodic migraine (EM) and chronic migraine (CM) based on headache frequency [3]. EM and CM are considered distinct pathophysiological entities that vary in terms of the frequency of headache episodes as well as the risks of medication overuse, comorbidities and treatment failures [4, 5]. Some unique neurovascular characteristics of CM have been proposed, including neurovascular coupling dysfunction [6], glymphatic disturbance [5, 7] and vascular impairments [8]. Changes in cerebral blood flow (CBF) across different stages of migraine have been reported in previous studies that used various approaches, including magnetic resonance imaging (MRI) [9, 10], cerebral angiography [11, 12], and single photon emission computed tomography [13]. However, these data remained inconclusive and the perfusion investigations of the phase-specific variance were scarce [14], or with limited sample size [15].

Arterial spin labeling (ASL) is a noninvasive technique in which MRI is used to evaluate intracranial perfusion [16]. By taking the advantage of magnetically labeled blood flow, ASL yields comparable outcomes of perfusion with isotope-labeling imaging [17] while avoiding the administration of isotopes or MRI contrasts. This technique has been used to investigate perfusion changes in several neurological disorders, including Alzheimer's disease [18], ischemic stroke [19], and cluster headache [20]. Some previous studies have used ASL to examine selected groups of migraine patients [21–25]; however, no consensus has been reached, and most of the studies had limited sample sizes [15, 21–23]. Therefore, there is a pressing need for comprehensive evaluations of the phasic and spatial perfusion dynamics in different subtypes and phases of migraine.

The primary outcome of this study was to examine the spatiotemporal dynamics of ASL perfusion in EM and CM patients. The secondary outcomes were to depict the differences of phase-specific dynamics of ASL perfusion between EM and CM, to delineate the potential clinical correlations of CBF with headache frequency, and to explore the potential values of CBF in specific anatomical locations in discriminating patients from controls. The ASL analysis in this study was conducted using a multifaceted approach, encompassing whole brain gray matter (GM) analysis, voxel-wise analysis, anatomical location analysis, and spatial similarity testing.

Methods

Ethics

The study protocol was approved by the Institutional Review Board of Taipei Veterans General Hospital (TVGH) (code 2021-02-018 C and 2023-06-024CC). All the investigations were performed in accordance with the principles of the Declaration of Helsinki, and all the subjects provided written informed consent before enrollment.

Study subjects

We recruited patients with migraine from the Headache Clinic at TVGH, a tertiary referral medical center with 3135 beds. The patients were recruited between 2021 and 2023. All migraine patients completed detailed headache questionnaires and neurological examinations. Patients were separated into EM (headache frequency < 15 days/month) and CM (≥ 15 days/month) groups based on the ICHD-3 criteria [3]. To eliminate the potential confounding's from medications, this study set a strict enrollment criterion to only recruit migraine subjects who were naïve to preventive medications. In addition, all participants were asked to refrain from painkillers for at least 2 days before the MR examinations. To further determine the disease phase of each subject, subjects completed telephone interviews 3 days after the MR exams to assess their headache status within these days. All the information was cross-checked with a prospectively recorded electronic headache diary. EM patients were further classified into preictal, ictal, postictal and interictal phases [26]. Detailed definitions of the EM and CM phases are listed in Supplementary Table 1. In patients with CM, those with no apparent distinction for ictal or interictal were classified as "unclassified" and were excluded from the phasic comparisons.

Healthy controls (HCs) were recruited from adjacent communities. Subjects with a known history of cancer, major neurological or psychiatric disorders, a history of intracranial operations, brain tumors, or a personal or family history (of second-degree relatives) of moderate or severe headache were not enrolled.

Imaging protocols

All brain images were acquired using a 3-Tesla (3T) MR machine (MR750, GE Healthcare, Milwaukee, WI) equipped with an eight-channel head coil. Initially, whole brain T1-weighted anatomical scans were obtained using a three-dimensional fluid-attenuated inversion-recovery fast spoiled gradient recalled echo pulse sequence with the following parameters: repetition time (TR)/echo time (TE)/inversion time (TI) = 9.4/4.0/450 milliseconds (ms), flip angle = 12°, field of view (FOV) = 256 × 256 mm, matrix size = 256 × 256, number of excitations (NEX) = 1, number of slices = 172, and slice thickness = 1.0 mm. Subsequently, ASL images were acquired using a pseudocontinuous ASL (pCASL) technique with a background-suppressed 3D fast spin echo sequence. The parameters for the pCASL technique were as follows: TR/TE/postlabel delay = 4632/10.5/1525 ms, FOV = 240 × 240 mm, matrix size = 128 × 128, NEX = 3, number of slices = 36, and slice thickness = 4.0 mm (ensuring whole brain coverage). For each participant, a CBF map was obtained based on both labeled (images taken shortly after the inflowing arterial spins were inverted) and unlabeled (images taken without inverting the arterial spins) ASL scans with the scanner console's FuncTool 3DASL (GE Healthcare) package and was reported in mL^{-1} 100 gm min^{-1} units. Additionally, 3D time-of-flight MR angiography (TOF-MRA; TR/TE = 25.00/2.90 ms; section thickness = 1 mm; multislab acquisitions) and T2-fluid-attenuated inversion-recovery (T2-FLAIR; TR/TE/TI = 6,000/128/1870 ms; slice thickness = 1 mm) images were obtained for each participant. Before image analysis, all images for each participant were visually evaluated by 2 experienced neuroradiologists (CHW and JFL) to exclude participants with intracranial space-occupying lesions, neurovascular disorders, gross brain abnormalities or insufficient image quality.

Image analysis

In this study, voxelwise comparisons of CBF between study groups were performed using Statistical Parametric Mapping software (SPM12, version 7771, Wellcome Institute of Neurology, University College London, UK, http://www.fil.ion.ucl.ac.uk/spm/) running in the MATLAB environment (version R2016a; MathWorks, Natick, MA). The analytical framework consisted of several steps. First, the unlabeled ASL scans were coregistered to the corresponding T1-weighted anatomical scans using the SPM Coregist function. The estimated transformation matrix obtained from this image registration process was subsequently applied to map the CBF maps into the T1-native space for each individual participant. Second, the T1-weighted anatomical scans were corrected for bias-field inhomogeneities, segmented into three distinct tissue types (GM, white matter (WM), and cerebrospinal fluid), and rigidly aligned to the standard Montreal Neurological Institute (MNI) space. Subsequently, the Diffeomorphic Anatomical Registration Through Exponentiated Lie algebra (DARTEL) toolbox was employed to construct study-specific tissue templates from all participants' rigidly aligned GM and WM tissue segments [27]. The obtained flow fields were used to warp the individual CBF maps to the standard MNI space and reslice them to an isotropic voxel size of 1.5 mm. To account for the partial volume effect (PVE), the individual CBF maps were corrected for tissue volume based on the proportion of GM and WM concentration in each voxel obtained from the segmented T1-weighted images [28]. Additionally, to eliminate potential outliers in the CBF maps due to large blood vessels or image preprocessing, voxels with CBF values lower than zero or higher than two standard deviations (SDs) above the mean CBF value were masked for each participant [29]. Finally, these PVE-corrected CBF maps were spatially smoothed using a 6-mm full width at half-maximum Gaussian kernel and subsequently utilized for statistical analyses.

Statistical analysis

This study was composed of three major investigative bundles: (1) phase-specific CBF alterations in EM, (2) phase-specific CBF alterations in CM, and (3) anatomical location and spatial pattern analysis of CBF. Clinical analysis examining the correlations between headache frequency and CBF in different EM and CM phases regarding the whole GM and other anatomical locations with significance in Bundles 1 and 2 was also conducted. Sex- and age-adjusted partial Pearson correlations between headache frequency and CBF values were also examined in those with complete records. The differences in demographic characteristics between the EM, CM and HC groups were assessed using the Pearson chi-squared test or independent samples t test, as appropriate. Descriptive statistics were reported as percentages or means ± SDs. For Bundle 1 analysis, whole brain GM CBF values were extracted from unsmoothed PVE-corrected CBF maps for each study group. Analysis of covariance (ANCOVA) was used to evaluate the mean GM CBF changes among the three study groups after adjusting for age and sex. Subsequently, a voxelwise, single-factor, three-level (HC, EM, and CM) ANCOVA design within the SPM12 general linear model framework, with age and sex as nuisance variables, was employed to assess voxelwise CBF alterations among the three study groups. For all voxelwise results, nonstationary cluster-level familywise error (FWE) correction was used to account for multiple comparisons, resulting in a cluster-defining threshold of $p < 0.005$ and a corrected cluster significance of FWE-corrected $p < 0.05$. Additionally, all unthresholded statistical maps were uploaded to the NeuroVault website and are available through a permanent link

(https://neurovault.org/collections/16749/). To identify potential phase-specific CBF alterations in patients with EM, global and voxelwise single-factor five-level (HC, EM-preictal, EM-ictal, EM-postictal, and EM-interictal) ANCOVA designs with the same nuisance variables were applied. Anatomical regions with significant between-group main effects based on the voxel-wise F-test were identified. These regions were further extracted, averaged, and used as input features for subsequent clinical association (headache frequency) and diagnostic discriminative capacity analyses. Receiver operating characteristic (ROC) curves were constructed for each anatomical region with significant EM-based phase-specific CBF alterations (four anatomical locations with significant results in voxelwise results) to evaluate its potential diagnostic discriminative capacity. For the combined anatomical panels of CBF in these four brain regions, a logistic regression model was applied to generate risk scores, and the discriminative capacity was further evaluated using the ROC curve. In Bundle 2, to identify potential phase-specific CBF alterations in CM patients, a single-factor, three-level (HC, CM-ictal, and CM-interictal) ANCOVA design was employed, with age and sex as nuisance covariates. The Bundle 3 analysis focused on the anatomical location and spatial patterns of the CBF differences between the EM and CM groups. We examined the previously identified clusters in Bundles 1 and 2 with significant CBF differences via post hoc analysis. The anatomical locations were further considered significant in Bundle 3 if they overlapped these clusters by at least 50% of the volume. We also investigated the spatial similarity of the CBF alteration patterns during the ictal phase between the EM and CM groups. Since our analyses in Bundles 1 and 2 revealed significant CBF changes during the ictal phase in both the EM and CM groups, we employed a spin permutation test to examine the spatial similarity of these alterations. Pearson correlation coefficients were first computed between the unthresholded t-statistic maps of the contrasts between the EM-ictal and EM-interictal groups and between the CM-ictal and CM-interictal groups. The significance of spatial similarity was further determined using a spatial spin permutation test approach involving 1,000 permutations. This method established a null distribution by comparing a target unthresholded t-statistic map with a permutated map generated by randomly rotating the spherical projections of the cortical surface while preserving the spatial relationships within the data [30]. The relevant code for conducting the spin permutation test is available at https://github.com/netneurolab/neuromaps. All non-voxelwise statistical analyses were performed using the Statistical Product and Service Solutions (IBM Corporation, Armonk, NY) statistics software package, version 24.0.

Results

Study subjects

A total of 297 migraine patients and 55 HCs were recruited (Supplementary Fig. 1). Two migraine patients were excluded due to incomplete clinical data. Since the CBF values in previous studies of migraine patients ranges from 52.7±6.9 to 59.7±10.6 [31] and those of HCs were approximately 50 [32], 6 subjects (1 EM patient+2 CM patients+3 HCs) with a CBF>90 or <30 were considered to be outliers and were thus excluded. Ultimately, 344 subjects (172 EM patients, 120 CM patients, and 52 HCs) were included for analysis.

The CBF values of the EM, CM and HC groups were analyzed. There were no differences in age or sex among the 3 groups (Table 1). No significant differences in whole brain GM CBF were detected between the EM, CM, and HC groups (Fig. 1). The voxelwise F test also did not reveal any significant differences in CBF between the EM, CM, and HC groups.

Bundle 1: phase-specific analysis in EM

EM patients (n=172) were further classified into preictal (n=30), ictal (n=35), postictal (n=42) and interictal (n=65) phases. The age (p=0.611), sex (p=0.570), aura presence (p=0.414), headache frequency (p=0.070) and MIDAS scores (p=0.316) were not different between EM subgroups (Table 2).

Table 1 Demographic characteristics of the study subjects

	Healthy controls (HCs)	Episodic migraine (EM) patients	Chronic migraine (CM) patients	*p*	*p* (EM vs. CM)
n	52	172	120	N/A	N/A
Age (yrs)	39.4±10.3	36.0±9.5	37.8±10.8	0.077	0.147
Sex (M/F)	19/33	38/134	25/95	0.064	0.797
Aura (1/0)	N/A	30/141	4/116	N/A	<0.001
Headache frequency (days/month)	N/A	3.5±3.2	21.3±6.9	N/A	<0.001
Onset age	N/A	19.1±6.9	21.6±9.6	N/A	0.013
MIDAS[a] scores	N/A	19.6±19.9	42.6±51.5	N/A	<0.001

[a]MIDAS = Migraine Disability Assessment

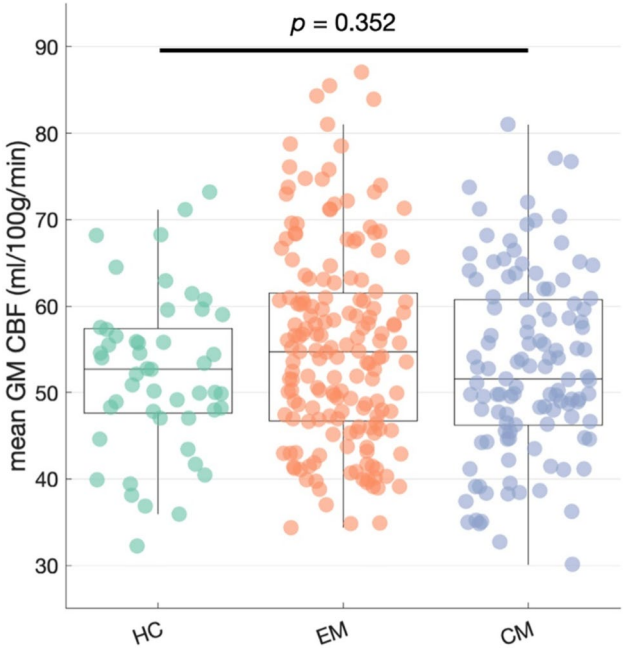

Fig. 1 No significant differences in CBF between episodic migraine (EM) patients, chronic migraine (CM) patients and healthy controls (HCs) were detected in the whole brain GM

We investigated the CBF changes between different EM phases. The whole GM CBF in the ictal phase was significantly higher than that in the other EM phases and in HCs after adjusting for sex and age ($p=0.038$; Fig. 2A). Voxelwise analysis further revealed that there were higher CBF values in the right planum temporale, left cerebellum crus II, right inferior temporal gyrus and left precuneus cortex in the ictal phase than in the other phases and in HCs (Fig. 2B). We further analyzed whether the CBF values of these four distinct anatomical locations could have diagnostic value. The combined anatomical panels of the CBF at these 4 locations had an area under the curve (AUC) of 0.780 (90% confidence interval; CI=0.674–0.886; $p<0.001$) for differentiating ictal EM patients from HCs and an AUC of 0.811 (90% CI=0.703–0.920; $p<0.001$) for differentiating ictal EM patients from preictal EM patients (Fig. 3).

Bundle 2: phase-specific analysis in CM

CM patients ($n=120$) were further classified into ictal ($n=67$), interictal ($n=31$) phases and unclassified ($n=22$). The age ($p=0.786$), sex ($p=0.073$), aura presence ($p=0.423$), headache frequency ($p=0.178$) and MIDAS scores ($p=0.556$) were not different between CM subgroups (Table 2).

We further analyzed whether CM patients also exhibited phasic changes in CBF. As some CM patients with nearly daily or daily attacks did not have obvious preictal, interictal or postictal phases, we compared only the whole GM and voxelwise CBF of patients with distinguishable interictal phases with patients during the ictal phase and HCs. Voxelwise analysis further revealed that CBF was higher in the right cerebellar crus II in the ictal phase than in the interictal phase and in the HCs after adjusting for sex and age (Fig. 2D). In contrast, no significant differences in the whole GM CBF were observed between the ictal subjects, interictal subjects and HCs (Fig. 2C).

Bundle 3: anatomical location and spatial analysis of voxelwise CBF

In Bundle 3, the anatomical location analysis was conducted by examining the clusters with significant CBF

Table 2 Major results of bundles 1 and 2 (the phasic analysis in the EM and CM groups)

Episodic migraine (EM) patients					
	Preictal	Ictal	Postictal	Interictal	*p*
n	30	35	42	65	
Age (yrs)	36.8 ± 9.4	37.6 ± 10.2	35.0 ± 9.1	35.5 ± 9.5	0.611
Sex (M/F)	6/24	5/30	10/32	17/48	0.570
Aura (1/0)	5/25	3/32	8/34	14/50	0.414
Headache frequency (days/month)	6.3 ± 3.3	7.8 ± 3.3	6.2 ± 3.3	6.1 ± 3.1	0.070
Onset age	21.5 ± 8.8	19.1 ± 6.8	17.3 ± 4.8	19.2 ± 7.1	0.095
MIDAS[a] scores	23.3 ± 20.4	23.1 ± 23.6	19.0 ± 24.1	16.5 ± 13.3	0.316
Chronic migraine (CM) patients					
	Ictal	Interictal	Unclassified	*p*	
n	67	31	22		
Age (yrs)	37.8 ± 11.3	36.8 ± 9.8	38.9 ± 10.9	0.786	
Sex (M/F)	9/58	10/21	6/16	0.073	
Aura (1/0)	2/65	2/29	0/22	0.423	
Headache frequency (days/month)	22.3 ± 6.7	19.6 ± 7.1	20.6 ± 7.2	0.178	
Onset age	22.1 ± 9.2	21.2 ± 9.3	20.5 ± 11.5	0.793	
MIDAS[a] scores	42.3 ± 54.3	36.6 ± 30.9	50.2 ± 65.1	0.556	

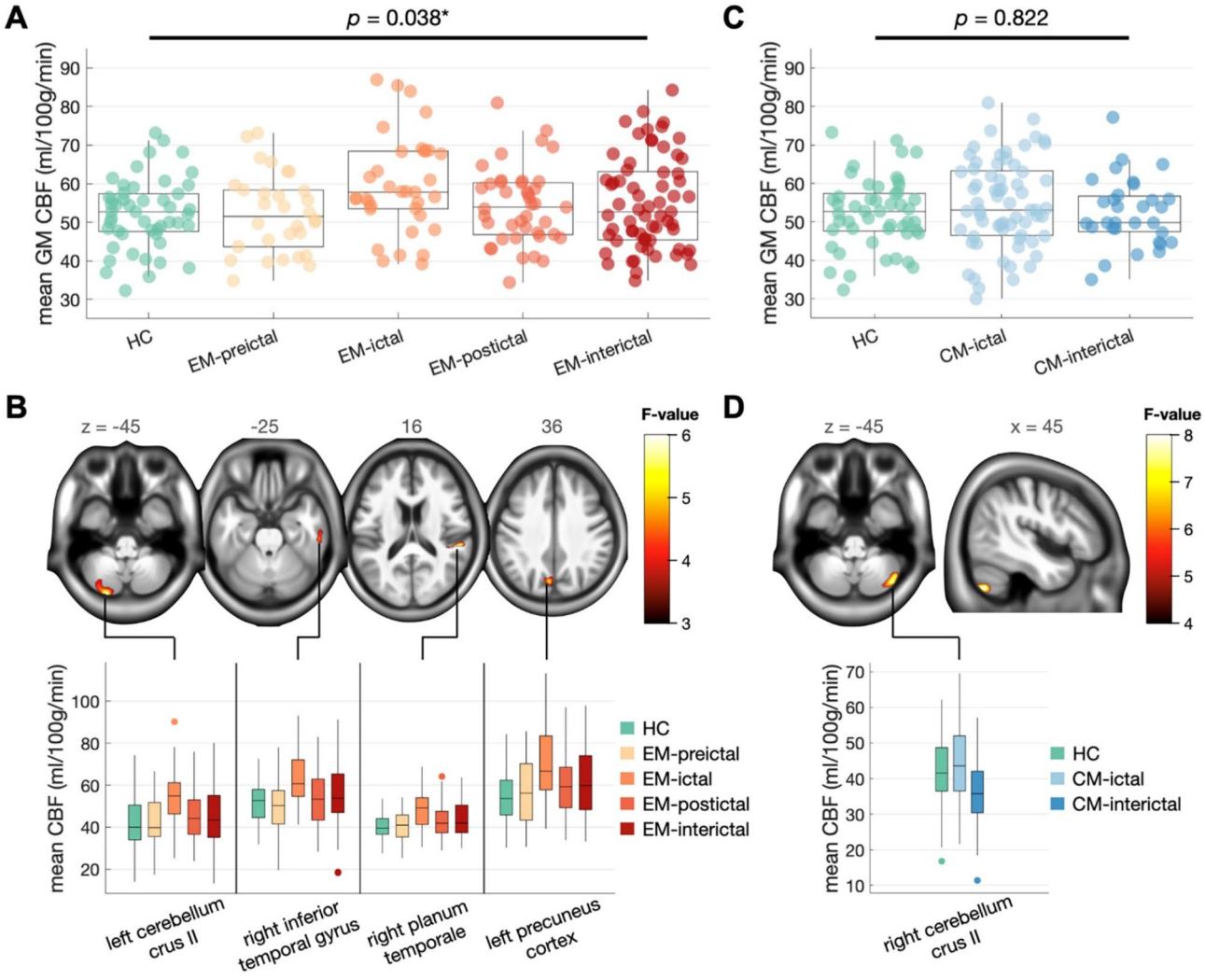

Fig. 2 Major results for Bundles 1 and 2. In Bundle 1 (episodic migraine; EM), (**A**) the whole gray matter (GM) cerebral blood flow (CBF) was higher in the ictal stage than in the other stages and in healthy controls (HCs). (**B**) Voxelwise analysis revealed that CBF was higher in the ictal stage than in the other stages at 4 anatomical locations (left cerebellum crus II, right inferior temporal gyrus, right planum temporale and left precuneus cortex). In Bundle 2 (chronic migraine; CM), (**C**) there were no significant differences in CBF between the ictal CM, interictal CM, unclassified CM and HC groups. (**D**) Voxelwise analysis revealed that CBF was higher in the ictal CM group than in the interictal CM group in the right cerebellar crus II

differences in the post hoc analysis for both Bundles 1 and 2. No significant differences in CBF were observed between the EM, CM and HC groups in terms of anatomical locations with ≥50% overlapping volume of each cluster (Supplementary Table 2). In EM subjects, higher CBF values occupying≥50% of the volume of each cluster were observed in the ictal phase than in the interictal phase in the following regions: right cerebellum VIIIa, VIIIb, IX, and crus II; bilateral frontal pole; bilateral temporal pole; left superior frontal gyrus; left paracingulate gyrus; left postcentral gyrus; and right superior parietal lobule. In CM subjects during the ictal phase, the CBF was higher than that in the subjects with interictal phase at right cerebellum crus II. Remarkably, the CBF in the right cerebellum crus II was even lower among the interictal CM patients than among the HCs.

Since the CBF was higher in both the EM and CM patients in the ictal phase in Bundles 1 and 2, we further examined the potential spatial differences in the CBF alteration patterns between the EM and CM subjects in the ictal phase by performing a spin permutation test. The spatial distributions of ictal-interictal CBF alterations in the EM and CM were not correlated with each other ($p=0.665$; $r=-0.018$; Supplementary Fig. 2).

Clinical analysis

To delineate the potential clinical impacts of CBF in migraine patients, we evaluated the correlations between CBF and headache frequency in all phases in terms of

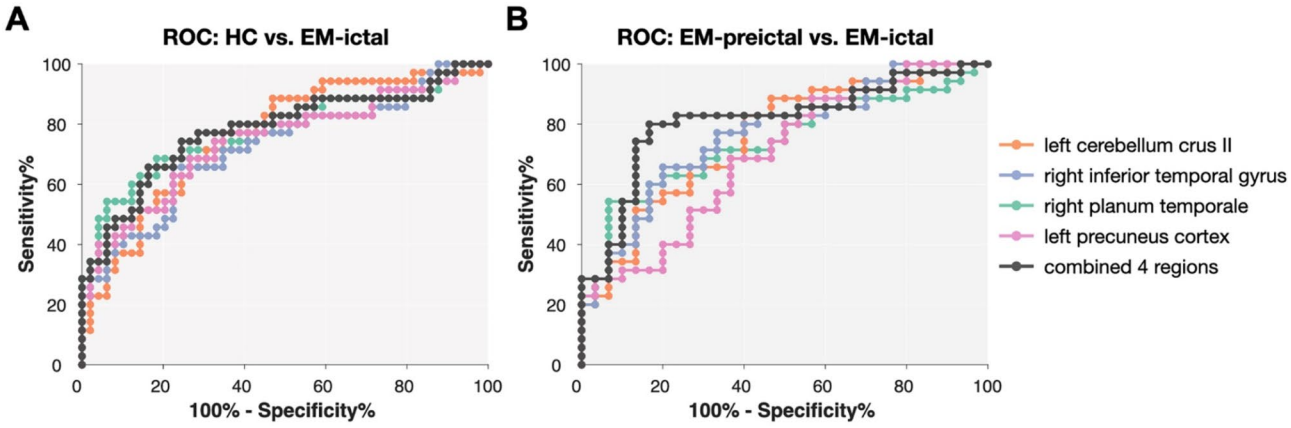

Fig. 3 Receiver operating characteristic (ROC) curves for the combined panels and 4 individual anatomical locations with higher cerebral blood flow (CBF) in ictal episodic migraine (EM) patients in Bundle 1. ROC curves for differentiating (**A**) ictal EM patients from HCs and (**B**) ictal EM patients from preictal EM patients were generated by analyzing the voxelwise CBF data in 4 anatomical locations (right planum temporale, left cerebellum crus II, right inferior temporal gyrus and left precuneus cortex) with higher CBF values among the ictal EM patients in Bundle 1

the whole GM and anatomical locations with significant differences in CBF between Bundles 1 and 2. CBF values were positively correlated with headache frequency after adjusting for age and sex in patients with ictal EM (p=0.044; r=0.353) and interictal CM (p=0.045; r=0.375) in the right inferior temporal gyrus as well as among patients with interictal CM in the left precuneus cortex (p=0.022; r=0.423) and the whole GM (p=0.010; r=0.470). No significant correlations were observed in the other phases regarding these anatomical locations (Supplementary Table 3).

Discussion

In this large-scale, prospective investigation, we examined the phasic dynamics of CBF in both EM and CM subjects. During the ictal phase, the CBF was significantly higher than that in the interictal phase in both EM and CM, with distinct involvement of specific anatomical locations. The composite model of CBF based on four anatomical locations was developed to distinguish the ictal phase from the preictal phase among patients with EM, and the discriminative capacity of the model exceeded 80%. Furthermore, while the CBF in the cerebellar crus II was significantly higher in the ictal phase in both the EM and CM patients, the spatial patterns of the changes in the ictal-interictal CBF differed between EM and CM patients. The unique CBF dynamics observed herein may help to elucidate the pathophysiology of migraines and help to differentiate different phases and subtypes of migraine.

The finding of higher ictal CBF in both EM and CM patients was parallel to the results of previous case series, which demonstrated regional hyperfusion in migraine patients during headache attacks [10, 33]; however, the CBF alteration pattern observed herein was not identical to that described in previous reports. Interestingly, increased CBF was detected in the cerebellum in both EM and CM patients in the ictal stage regardless of whether voxelwise or anatomical location analysis was performed, suggesting that this could be a disease signature across different phenotypes. Previous studies have indicated the potential role of the cerebellum in the pathophysiology of migraines [34] and revealed the impacts of structural [35, 36] and functional changes [37–39] in the cerebellum. Cerebellar volume was smaller in patients with migraine [36], and exacerbated atrophy was observed in CM patients [35]. The cerebellum also plays a significant role in brain functions in trigeminal nociception [38, 39]. Remarkably, the right cerebellar crus II, which presented as the only region with increased CBF in the CM in Bundle 2, has been shown to have increased GM volume in migraine patients [37]. Furthermore, this specific anatomical location was associated with higher levels of neural activity, which are strongly correlated with cerebral perfusion (especially CBF) [40, 41], during nociception in the ictal phase among migraine patients [37]. Our previous study also revealed that the outcomes of patients with high-frequency migraine were associated with increased GM volume in the cerebellum [42]. Additionally, dysfunction of the cerebellar crus II is potentially associated with a decreased response to the limbic system, which is often impaired in migraine patients [43]. Taken together, these data indicated that cerebellar crus II may play a significant role in pathophysiology of migraines and even the chronification migraines. Repetitive ictal hyperperfusion may contribute to long-term structural or connectivity alterations, although the causal links have yet to be fully elucidated.

The combined panels of the CBF from four distinct anatomical locations identified from voxelwise analysis demonstrated good discriminative capacity for differentiating ictal EM from preictal EM and HCs. These results

not only indicated that CBF could be a reliable imaging biomarker for differentiating the ictal phase from other phases but also had pathophysiological implications. The significant increase in CBF from the preictal phase to the ictal phase suggests that these four anatomical locations actively participate in the pathogenic processes of migraine and potentially reflect how the brain responds to or engages in the activation of the trigeminovascular system. In addition to the abovementioned cerebellar crus II, previous studies have reported increased levels of functional activity in the planum temporale [44], right temporal gyrus [45], and left precuneus cortex [46] among patients with migraine or its subtypes [45]. These phenomena may indicate a potential correlation between regional hyperperfusion and increased functional connectivity. The CBF was also higher in CM patients during the ictal phase than in CM patients during the interictal phase; however, the CBF in CM patients in the interictal phase was lower than that among controls. We hypothesized that during the process of migraine chronification, each individual attack could lead to plastic changes in the brain. Although ictal hyperperfusion persists in CM patients, the interictal brain may require less CBF owing to chronic dysfunction of neural circuitry or reactive gliosis. In fact, regarding the whole brain GM, the interictal CM was the only phase with a positive correlation between headache frequency and CBF. This phenomenon further supported the potentially unique plastic changes along with migraine chronification. Moreover, recent studies in humans [5] and mice [7] revealed potential glymphatic dysfunctions in CM and indicated a potential relationship between CBF and glymphatic functions [47]. Therefore, we speculated that CM subjects may have long-term CBF dysregulation, and future research should examine the potential contributions of CBF to the known glymphatic dysfunctions among CM patients [5, 7].

Further delineation of perfusion dynamics differences between CM patients and EM patients is important for identifying pathophysiological differences in patients with different headache frequencies. Although the CBF values were similar between CM and EM as a group in Bundle 1, our data indicated that these 2 different patient groups (EM and CM patients) may exhibit differences in terms of the ictal-interictal transformation of perfusion dynamics. Furthermore, the positive correlation between interictal CM and CBF regarding the whole brain GM and other anatomical locations revealed the fundamental differences in brain perfusion between the EM and CM groups. Previous studies revealed the characteristic interictal functional status in frontal [48] and fronto-occipital [49] areas of the brain. Our previous study also revealed differences in GM functional connectivity between EM and CM patients [50]. Although further research is necessary to elucidate the potential effects of whole GM perfusion pattern alterations during chronification, our findings suggest that fundamental perfusion differences between EM and CM patients exist in the ictal-interictal CBF spatial distribution.

Strengths and limitations

This study had several strengths. First, this was a large-scale ($n=344$) prospective study. All the subjects, including the migraine patients and HCs, underwent a standardized imaging protocol on the same 3T MRI machine. Detailed subgroups of migraine patients by disease phases and sex- and age-adjusted evaluations between the migraine subgroups and HCs provided substantial evidence of the perfusion dynamics in the disease. All the diagnoses and phenotyping of migraine patients were conducted by experienced headache specialists. Finally, all migraine subjects were naïve to preventive medications and refrained from analgesics 2 days before the MRI; therefore, the potential confounders of brain perfusion by medications were minimized.

However, there were some limitations in this study. We did not strictly control blood pressure in the study subjects. Although a previous study revealed that blood pressure changes did not contribute to CBF alterations in selected patients [51], and the correlations between migraine and hypertension remain controversial [52], potentially minimal effects of blood pressure changes on brain perfusion may exist. However, most of our patients were otherwise healthy without hypertension or other cardiovascular risk factors. In addition, since there were no significant changes in blood pressure upon MR examination compared to baseline, we believe that the effects were minimal. Finally, we did not perform additional dynamic contrast-enhanced MRI (DCE-MRI) to evaluate brain perfusion in this study to avoid unnecessary administration of gadolinium-based contrast agents in patients, especially HCs [53]. With the similar diagnostic accuracy of ASL and DCE-MRI in brain perfusion [54], we believe that the perfusion evaluations by ASL in this study were evident. Finally, some clinical characteristics, including headache frequency, may be confounding factors for phasic investigations. However, through clinical investigations, we demonstrated that whole brain GM CBF was not correlated with headache frequency in any phase. Although further studies may be needed to determine the potential effects of all clinical characteristics in different migraine phases, the potential effects of frequency on CBF may be limited in this study.

Conclusions

Higher CBF in the ictal stages of EM and CM and the distinct spatial distributions of whole GM CBF dynamics between EM and CM patients were observed herein. The findings revealed the role of CBF as an imaging marker

for differentiating the ictal stage of migraines from other stages, especially among subjects with ictal EM. Furthermore, the results revealed potential pathogenic mechanisms of migraine.

Abbreviations

ANOVA	Analysis of covariance
ASL	Arterial spin labeling
CBF	Cerebral blood flow
CM	Chronic migraine
DARTEL	Diffeomorphic Anatomical Registration Through Exponentiated Lie algebra
EM	Episodic migraine
FOV	Field of view
GM	Gray matter
HC	Healthy control
MNI	Montreal Neurological Institute
MRI	Magnetic resonance imaging
NEX	Number of excitations
PVE	Partial volume effect
pCASL	Pseudocontinuous arterial spin labeling
ROC	Receiver operating characteristic
SD	Standard deviation
T	Tesla
TE	Echo time
TI	Inversion time
TOF-MRA	Time-of-flight magnetic resonance angiography
TR	Repetition time
TVGH	Taipei Veterans General Hospital
T2-FLAIR	T2-fluid-attenuated inversion-recovery

Supplementary Information

The online version contains supplementary material available at https://doi.org/10.1186/s10194-024-01880-6.

Supplementary Material 1

Acknowledgements

This work was supported by the Brain Research Center, National Yang Ming Chiao Tung University from The Featured Areas Research Center Program within the framework of the Higher Education Sprout Project by the Ministry of Education (MOE) in Taiwan (to SJW & SPC); the National Science and Technology Council, Taiwan [NSTC 108-2314-B-010-022 -MY3, 110-2326-B-A49A-501-MY3 & 112-2314-B-A49-037-MY3 (to SPC); 110-2321-B-010-005-, 111-2321-B-A49-004, 111-2321-B-A49-011, 111-2314-B-A49-069-MY3, 111-2314-B-075-086-MY3, 111-2314-B-A49-090-MY3 & 112-2321-B-075-007 (to SJW); 113-2314-B-A49-070- & 112-2314-B-A49-056- (to KHC); 111-2314-B-075-025 -MY3 & 110-2314-B-075-005 (to CHW)], Ministry of Health and Welfare, Taiwan [MOHW107-TDU-B-211-123001, MOHW 108-TDU-B-211-133001 and MOHW112-TDU-B-211-144001] (to SJW), and Taipei Veterans General Hospital, Taiwan [V113C-120, V113E004-1, V112C-113 & V112E-004-1 (to SJW); V112D67-001-MY3-2 & V113C-058 (to SPC); V112B-007 (to CHW)], Veterans General Hospitals and University System of Taiwan Joint Research Program [VGHUST-112-G1-2-1 (to SJW)]; Yen Tjing Ling Medical Foundation [CI-112-2 (to CHW)], Professor Tsuen CHANG's Scholarship Program from Medical Scholarship Foundation In Memory Of Professor Albert Ly-Young Shen (to CHW), Vivian W. Yen Neurological Foundation (to CHW), Yin Shu-Tien Foundation Taipei Veterans General Hospital-National Yang Ming Chiao Tung University Excellent Physician Scientists Cultivation Program, [No.112-V-B-039; No. 113-V-B-020 (to CHW)]. The funders have no roles in the conceptualization, design, data collection, analysis, decision to publish, or preparation of the manuscript.

Author contributions

KHC, SPC and SJW contributed to the conception and design of the study. CHW, PLL, YFW, JFL, STC and CJL acquired and analyzed the data. CHW, PLL, YFW and JFL were major contributors in writing the manuscript. All authors read and approved the final manuscript.

Funding

This work was supported by the Brain Research Center, National Yang Ming Chiao Tung University from The Featured Areas Research Center Program within the framework of the Higher Education Sprout Project by the Ministry of Education (MOE) in Taiwan (to SJW & SPC); the National Science and Technology Council, Taiwan [NSTC 108-2314-B-010-022 -MY3, 110-2326-B-A49A-501-MY3 & 112-2314-B-A49-037-MY3 (to SPC); 110-2321-B-010-005-, 111-2321-B-A49-004, 111-2321-B-A49-011, 111-2314-B-A49-069-MY3, 111-2314-B-075-086-MY3, 111-2314-B-A49-090-MY3 & 112-2321-B-075-007 (to SJW); 113-2314-B-A49-070- & 112-2314-B-A49-056- (to KHC); 111-2314-B-075-025 -MY3 & 110-2314-B-075-005 (to CHW)], Ministry of Health and Welfare, Taiwan [MOHW107-TDU-B-211-123001, MOHW 108-TDU-B-211-133001 and MOHW112-TDU-B-211-144001] (to SJW), and Taipei Veterans General Hospital, Taiwan [V113C-120, V113E004-1, V112C-113 & V112E-004-1 (to SJW); V112D67-001-MY3-2 & V113C-058 (to SPC); V112B-007 (to CHW)], Veterans General Hospitals and University System of Taiwan Joint Research Program [VGHUST-112-G1-2-1 (to SJW)]; Yen Tjing Ling Medical Foundation [CI-112-2 (to CHW)], Professor Tsuen CHANG's Scholarship Program from Medical Scholarship Foundation In Memory Of Professor Albert Ly-Young Shen (to CHW), Vivian W. Yen Neurological Foundation (to CHW), Yin Shu-Tien Foundation Taipei Veterans General Hospital-National Yang Ming Chiao Tung University Excellent Physician Scientists Cultivation Program, [No.112-V-B-039; No. 113-V-B-020 (to CHW)]. The funders have no roles in the conceptualization, design, data collection, analysis, decision to publish, or preparation of the manuscript.

Data availability

All unthresholded statistical maps were uploaded to the NeuroVault website and are available through a permanent link (https://neurovault.org/collections/16749/).

Declarations

Ethics approval and consent to participate

All study subjects provided written informed consent before enrollment, and the study protocols were approved by the Institutional Review Board of Taipei Veterans General Hospital (TVGH) (code 2021-02-018 C and 2023-06-024CC). All investigations were conducted according to the principles of the Declaration of Helsinki.

Consent for publication

Not applicable.

Competing interests

SPC has served as an Associate Editor of TJHP and the Guest Editor of the collection "Vascular Triggers of Headache Disorders" in TJHP.

Author details

[1]Department of Radiology, Taipei Veterans General Hospital, Taipei, Taiwan
[2]School of Medicine, National Yang Ming Chiao Tung University, Taipei, Taiwan
[3]Center for Healthy Longevity and Aging Sciences, National Yang Ming Chiao Tung University, Taipei, Taiwan
[4]Department of Neurology, Neurological Institute, Taipei Veterans General Hospital, No. 201, Sec. 2, Shipai Rd., Beitou District, Taipei 11217, Taiwan
[5]Brain Research Center, National Yang Ming Chiao Tung University, No. 155, Sec. 2, Linong St. Beitou Dist., Taipei 112304, Taiwan
[6]Institute of Neuroscience, National Yang Ming Chiao Tung University, Taipei, Taiwan
[7]Institute of Clinical Medicine, National Yang Ming Chiao Tung University, Taipei, Taiwan
[8]Division of Translational Research, Department of Medical Research, Taipei Veterans General Hospital, Taipei, Taiwan

Received: 23 August 2024 / Accepted: 27 September 2024
Published online: 03 October 2024

References

1. Steiner TJ, Stovner LJ (2023) Global epidemiology of migraine and its implications for public health and health policy. Nat Rev Neurol 19(2):109–117. https://doi.org/10.1038/s41582-022-00763-1
2. GBD 2016 Disease and Injury Incidence and Prevalence Collaborators (2017) Global, regional, and national incidence, prevalence, and years lived with disability for 328 diseases and injuries for 195 countries, 1990–2016: a systematic analysis for the global burden of Disease Study 2016. Lancet 390(10100):1211–1259. https://doi.org/10.1016/S0140-6736(17)32154-2
3. Headache Classification Committee of the International Headache Society (IHS). Headache classification committee of the international headache society (IHS) the international classification of headache disorders, 3rd edition. Cephalalgia (2018) https://doi.org/10.1177/0333102417738202
4. May A, Schulte LH (2016) Chronic migraine: risk factors, mechanisms and treatment. Nat Rev Neurol 12(8):455–464. https://doi.org/10.1038/nrneurol.2016.93
5. Wu CH, Chang FC, Wang YF, Lirng JF, Wu HM, Pan LH et al (2023) Impaired glymphatic and meningeal lymphatic functions in patients with chronic migraine. Ann Neurol 95(3):583–595. https://doi.org/10.1002/ana.26842
6. Hu B, Yu Y, Dai YJ, Feng JH, Yan LF, Sun Q et al (2019) Multi-modal MRI reveals the neurovascular coupling dysfunction in chronic migraine. Neuroscience 419:72–82. https://doi.org/10.1016/j.neuroscience.2019.09.022
7. Huang W, Zhang Y, Zhou Y, Zong J, Qiu T, Hu L et al (2023) Glymphatic dysfunction in migraine mice model. Neuroscience 528:64–74. https://doi.org/10.1016/j.neuroscience.2023.07.027
8. Caballero PEJ, Escudero FM (2013) Peripheral endothelial function and arterial stiffness in patients with chronic migraine: a case-control study. J Headache Pain 14(1):8. https://doi.org/10.1186/1129-2377-14-8
9. Russo A, Silvestro M, Tessitore A, Orologio I, De Rosa AP, De Micco R et al (2023) Arterial spin labeling MRI applied to migraine: current insights and future perspectives. J Headache Pain 24(1):71. https://doi.org/10.1186/s10194-023-01597-y
10. Pollock JM, Deibler AR, Burdette JH, Kraft RA, Tan H, Evans AB et al (2008) Migraine associated cerebral hyperperfusion with arterial spin-labeled MR imaging. AJNR Am J Neuroradiol 29(8):1494–1497. https://doi.org/10.3174/ajnr.A1115
11. Friberg L, Olesen J, Lassen NA, Olsen TS, Karle A (1994) Cerebral oxygen extraction, oxygen consumption, and regional cerebral blood flow during the aura phase of migraine. Stroke 25(5):974–979. https://doi.org/10.1161/01.str.25.5.974
12. Olesen J, Friberg L, Olsen TS, Iversen HK, Lassen NA, Andersen AR et al (1990) Timing and topography of cerebral blood flow, aura, and headache during migraine attacks. Ann Neurol 28(6):791–798. https://doi.org/10.1002/ana.410280610
13. Ferrari MD, Haan J, Blokland JA, Arndt JW, Minnee P, Zwinderman AH et al (1995) Cerebral blood flow during migraine attacks without aura and effect of sumatriptan. Arch Neurol 52(2):135–139. https://doi.org/10.1001/archneur.1995.00540260037013
14. Karsan N, Goadsby PJ (2023) Neuroimaging in the pre-ictal or premonitory phase of migraine: a narrative review. J Headache Pain 24(1):106. https://doi.org/10.1186/s10194-023-01617-x
15. Arkink EB, Bleeker EJ, Schmitz N, Schoonman GG, Wu O, Ferrari MD et al (2012) Cerebral perfusion changes in migraineurs: a voxelwise comparison of interictal dynamic susceptibility contrast MRI measurements. Cephalalgia 32(4):279–288. https://doi.org/10.1177/0333102411435985
16. Haller S, Zaharchuk G, Thomas DL, Lovblad KO, Barkhof F, Golay X (2016) Arterial spin labeling perfusion of the brain: emerging clinical applications. Radiology 281(2):337–356. https://doi.org/10.1148/radiol.2016150789
17. Puig O, Henriksen OM, Vestergaard MB, Hansen AE, Andersen FL, Ladefoged CN et al (2020) Comparison of simultaneous arterial spin labeling MRI and (15)O-H(2)o PET measurements of regional cerebral blood flow in rest and altered perfusion states. J Cereb Blood Flow Metab 40(8):1621–1633. https://doi.org/10.1177/0271678X19874643
18. Alsop DC, Detre JA, Golay X, Gunther M, Hendrikse J, Hernandez-Garcia L et al (2015) Recommended implementation of arterial spin-labeled perfusion MRI for clinical applications: a consensus of the ISMRM perfusion study group and the European consortium for ASL in dementia. Magn Reson Med 73(1):102–116. https://doi.org/10.1002/mrm.25197
19. de Havenon A, Haynor DR, Tirschwell DL, Majersik JJ, Smith G, Cohen W et al (2017) Association of collateral blood vessels detected by arterial spin labeling magnetic resonance imaging with neurological outcome after ischemic stroke. JAMA Neurol 74(4):453–458. https://doi.org/10.1001/jamaneurol.2016.4491
20. Wei DY, O'Daly O, Zelaya FO, Goadsby PJ (2022) Areas of cerebral blood flow changes on arterial spin labelling with the use of symmetric template during nitroglycerin triggered cluster headache attacks. Neuroimage Clin 33:102920. https://doi.org/10.1016/j.nicl.2021.102920
21. Giani L, Lovati C, Corno S, Lagana MM, Baglio F, Mariani C (2019) Cerebral blood flow in migraine without aura: ASL-MRI case control study. Neurol Sci 40(Suppl 1):183–184. https://doi.org/10.1007/s10072-019-03806-6
22. Michels L, Villanueva J, O'Gorman R, Muthuraman M, Koirala N, Buchler R et al (2019) Interictal hyperperfusion in the higher visual cortex in patients with episodic migraine. Headache 59(10):1808–1820. https://doi.org/10.1111/head.13646
23. Wolf ME, Okazaki S, Eisele P, Rossmanith C, Gregori J, Griebe M et al (2018) Arterial spin labeling cerebral perfusion magnetic resonance imaging in migraine aura: an observational study. J Stroke Cerebrovasc Dis 27(5):1262–1266. https://doi.org/10.1016/j.jstrokecerebrovasdis.2017.12.002
24. Fu T, Liu L, Huang X, Zhang D, Gao Y, Yin X et al (2022) Cerebral blood flow alterations in migraine patients with and without aura: an arterial spin labeling study. J Headache Pain 23(1):131. https://doi.org/10.1186/s10194-022-01501-0
25. Schramm S, Borner C, Reichert M, Hoffmann G, Kaczmarz S, Griessmair M et al (2024) Perfusion imaging by arterial spin labeling in migraine: a literature review. J Cereb Blood Flow Metab 44(8):1253–1270. https://doi.org/10.1177/0271678X241237733
26. Peng KP, May A (2020) Redefining migraine phases - a suggestion based on clinical, physiological, and functional imaging evidence. Cephalalgia 40(8):866–870. https://doi.org/10.1177/0333102419898868
27. Ashburner J (2007) A fast diffeomorphic image registration algorithm. NeuroImage 38(1):95–113. https://doi.org/10.1016/j.neuroimage.2007.07.007
28. Johnson NA, Jahng GH, Weiner MW, Miller BL, Chui HC, Jagust WJ et al (2005) Pattern of cerebral hypoperfusion in Alzheimer disease and mild cognitive impairment measured with arterial spin-labeling MR imaging: initial experience. Radiology 234(3):851–859. https://doi.org/10.1148/radiol.2343040197
29. Wang Z, Aguirre GK, Rao H, Wang J, Fernandez-Seara MA, Childress AR et al (2008) Magn Reson Imaging 26(2):261–269. https://doi.org/10.1016/j.mri.2007.07.003. Empirical optimization of ASL data analysis using an ASL data processing toolbox: ASLtbx
30. Alexander-Bloch AF, Shou H, Liu S, Satterthwaite TD, Glahn DC, Shinohara RT et al (2018) On testing for spatial correspondence between maps of human brain structure and function. NeuroImage 178:540–551. https://doi.org/10.1016/j.neuroimage.2018.05.070
31. Bednarczyk EM, Remler B, Weikart C, Nelson AD, Reed RC (1998) Global cerebral blood flow, blood volume, and oxygen metabolism in patients with migraine headache. Neurology 50(6):1736–1740. https://doi.org/10.1212/wnl.50.6.1736
32. Lassen NA (1985) Normal average value of cerebral blood flow in younger adults is 50 ml/100 g/min. J Cereb Blood Flow Metab 5(3):347–349. https://doi.org/10.1038/jcbfm.1985.48
33. Chen Z, Chen X, Liu M, Liu M, Ma L, Yu S (2018) Evaluation of gray matter perfusion in episodic migraine using voxel-wise comparison of 3D pseudo-continuous arterial spin labeling. J Headache Pain 19(1):36. https://doi.org/10.1186/s10194-018-0866-y
34. Vincent M, Hadjikhani N (2007) The cerebellum and migraine. Headache 47(6):820–833. https://doi.org/10.1111/j.1526-4610.2006.00715.x
35. Demir BT, Bayram NA, Ayturk Z, Erdamar H, Seven P, Calp A et al (2016) Structural changes in the cerebrum, cerebellum and corpus callosum in migraine patients. Clin Invest Med 39(6):27495
36. Qin Z, He XW, Zhang J, Xu S, Li GF, Su J et al (2019) Structural changes of cerebellum and brainstem in migraine without aura. J Headache Pain 20(1):93. https://doi.org/10.1186/s10194-019-1045-5
37. Mehnert J, May A (2019) Functional and structural alterations in the migraine cerebellum. J Cereb Blood Flow Metab 39(4):730–739. https://doi.org/10.1177/0271678X17722109
38. Stankewitz A, Voit HL, Bingel U, Peschke C, May A (2010) A new trigeminonociceptive stimulation model for event-related fMRI. Cephalalgia 30(4):475–485. https://doi.org/10.1111/j.1468-2982.2009.01968.x
39. Mehnert J, Schulte L, Timmann D, May A (2017) Activity and connectivity of the cerebellum in trigeminal nociception. NeuroImage 150:112–118. https://doi.org/10.1016/j.neuroimage.2017.02.023
40. He F, Sullender CT, Zhu H, Williamson MR, Li X, Zhao Z et al (2020) Multimodal mapping of neural activity and cerebral blood flow reveals long-lasting

neurovascular dissociations after small-scale strokes. Sci Adv. ;6(21):eaba1933. https://doi.org/10.1126/sciadv.aba1933
41. Thompson JK, Peterson MR, Freeman RD (2003) Single-neuron activity and tissue oxygenation in the cerebral cortex. Science 299(5609):1070–1072. https://doi.org/10.1126/science.1079220
42. Liu HY, Lee PL, Chou KH, Lai KL, Wang YF, Chen SP et al (2020) The cerebellum is associated with 2-year prognosis in patients with high-frequency migraine. J Headache Pain 21(1):29. https://doi.org/10.1186/s10194-020-01096-4
43. Wei HL, Chen J, Chen YC, Yu YS, Zhou GP, Qu LJ et al (2020) Impaired functional connectivity of limbic system in migraine without aura. Brain Imaging Behav 14(5):1805–1814. https://doi.org/10.1007/s11682-019-00116-5
44. Dobos D, Kokonyei G, Gyebnar G, Szabo E, Kocsel N, Galambos A et al (2023) Microstructural differences in migraine: a diffusion-tensor imaging study. Cephalalgia 43(12):3331024231216456. https://doi.org/10.1177/03331024231216456
45. Li ZY, Si LH, Shen B, Ling X, Yang X (2023) Altered functional activity in the right superior temporal gyrus in patients with definite vestibular migraine. Neurol Sci 44(5):1719–1729. https://doi.org/10.1007/s10072-022-06570-2
46. Wu L, Wang X, Liu Q, Chai L, Tian S, Wu W (2023) A study on alterations in functional activity in migraineurs during the interictal period. Heliyon 9(1):e12372. https://doi.org/10.1016/j.heliyon.2022.e12372
47. Kylkilahti TM, Berends E, Ramos M, Shanbhag NC, Toger J, Bloch KM et al (2021) Achieving brain clearance and preventing neurodegenerative diseases-A glymphatic perspective. J Cereb Blood Flow Metab 41(9):2137–2149. https://doi.org/10.1177/0271678X20982388
48. Wu D, Zhou Y, Xiang J, Tang L, Liu H, Huang S et al (2016) Multi-frequency analysis of brain connectivity networks in migraineurs: a magnetoencephalography study. J Headache Pain 17:38. https://doi.org/10.1186/s10194-016-0636-7
49. Cao Z, Lin CT, Chuang CH, Lai KL, Yang AC, Fuh JL et al (2016) Resting-state EEG power and coherence vary between migraine phases. J Headache Pain 17(1):102. https://doi.org/10.1186/s10194-016-0697-7
50. Hsiao FJ, Chen WT, Liu HY, Wang YF, Chen SP, Lai KL et al (2021) Migraine chronification is associated with beta-band connectivity within the pain-related cortical regions: a magnetoencephalographic study. Pain 162(10):2590–2598. https://doi.org/10.1097/j.pain.0000000000002255
51. Foster-Dingley JC, Moonen JE, de Craen AJ, de Ruijter W, van der Mast RC, van der Grond J (2015) Blood pressure is not associated with cerebral blood flow in older persons. Hypertension 66(5):954–960. https://doi.org/10.1161/HYPERTENSIONAHA.115.05799
52. Wang YF, Wang SJ (2021) Hypertension and migraine: time to revisit the evidence. Curr Pain Headache Rep 25(9):58. https://doi.org/10.1007/s11916-021-00976-x
53. Robert P, Fingerhut S, Factor C, Vives V, Letien J, Sperling M et al (2018) One-year retention of gadolinium in the brain: comparison of gadodiamide and gadoterate meglumine in a rodent model. Radiology 288(2):424–433. https://doi.org/10.1148/radiol.2018172746
54. Lavrova A, Teunissen WHT, Warnert EAH, van den Bent M, Smits M (2022) Diagnostic accuracy of arterial spin labeling in comparison with dynamic susceptibility contrast-enhanced perfusion for brain tumor surveillance at 3T MRI. Front Oncol 12:849657. https://doi.org/10.3389/fonc.2022.849657

Publisher's note